PROCEEDINGS OF SCIENCE

The Radio Neutrino Observatory Greenland (RNO-G): Status update

Steffen Hallmann[a,*] **for the RNO-G Collaboration**

(a complete list of authors can be found at the end of the proceedings)

[a] *Deutsches Elektronen-Synchrotron (DESY), Platanenallee 6, 15738 Zeuthen, Germany*

E-mail: steffen.hallmann@desy.de

The Radio Neutrino Observatory in Greenland (RNO-G) is an in-ice radio detector for ultra-high energy neutrinos with the potential to make the first detection of a neutrino shower beyond ~10 PeV via the Askaryan emission. With a projected 90% CL upper limit below $E^2\Phi \approx 10^{-8}\,\mathrm{GeV/cm^2/s/sr}$ within 10 years of operation, RNO-G will reach realistic models of GZK and astrophysical neutrino fluxes. In 2021, the first three stations of RNO-G were installed and started data-taking. Four additional stations were added in 2022 with some upgrades to the station hardware. Here, we present the current status of the instrument and give an overview of the efforts towards calibration and analysis of the data recorded so far.

9th International Workshop on Acoustic and Radio EeV Neutrino Detection Activities - ARENA2022
7-10 June 2022
Santiago de Compostela, Spain

*Speaker

PoS(ARENA2022)005

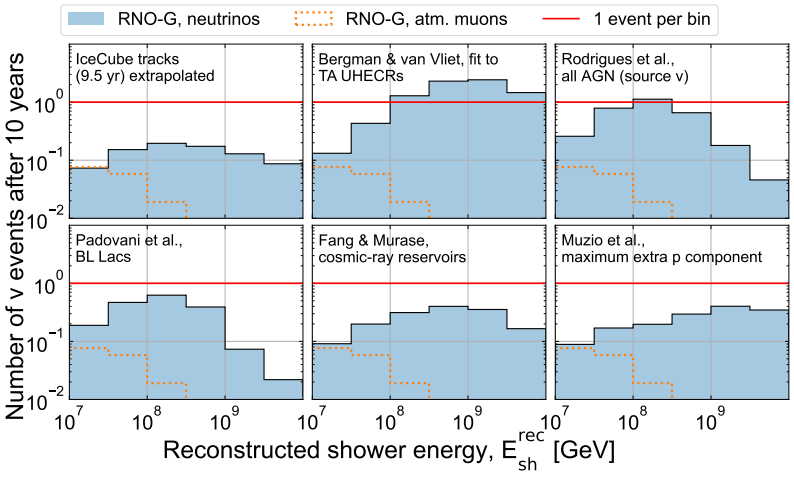

Figure 1: Expected number of events after 10 years (assuming 66% up-time from solar power) operation with a completed RNO-G detector. Several of the models shown [9–14] project a total event count $\gtrsim 1$ in RNO-G.

1. Scope of RNO-G

The IceCube neutrino observatory has discovered the diffuse extragalactic astrophysical neutrino flux [1] at TeV to PeV energies, and with the recent identification of TXS 0506+056 and NGC 1068 as two likely point sources [2, 3] it is just sensitive enough to herald the era of neutrino astronomy. However, the short attenuation length of optical signals in ice and water prevents scaling the established optical Cherenkov detectors to the size which would be necessary to counter the falling flux with energy in order to extend the accessible energy region beyond ~10 PeV.

The Radio Neutrino Observatory in Greenland (RNO-G) [4] is a neutrino detector under construction using the radio detection technique to detect ultra-high-energy (UHE) neutrinos with energies beyond 3×10^{16} eV via Askaryan emission. The Askaryan radio signal is generated in the particle cascades of UHE neutrino interactions in ice and has an impulsive and coherent cone-shaped emission profile. Building on the (amongst others) pioneering ARIANNA, ARA and ANITA experiments (cf. Ref. [5] for a review), RNO-G is the first mid-sized array implementation of the radio detection technique. It will consist of 35 detector stations distributed over an area of $\sim 50\,\mathrm{km}^2$. With an expected 90% CL upper limit below $E^2\Phi \approx 10^{-8}\,\mathrm{GeV/cm^2/s/sr}$ after 10 years of operation [4], RNO-G is large enough such that realistic ultra-high-energy (UHE) neutrino flux models come into reach. The expected number of events for the models shown in Fig. 1 suggests that RNO-G is likely to make the first ever neutrino detection using the radio technique.

In addition to the prospect of detecting in-ice neutrinos, RNO-G also covers a large surface area for detecting cosmic-ray (CR) air-showers. Already the seven out of 35 stations deployed so far are recording a few CR events per day, even for a conservative trigger threshold [6]. These CR events not only serve as a valuable validation signal, but can also be used to probe cosmic-ray flux and interaction models [7]. In addition, RNO-G serves as a development platform to inform the design of a $\sim 10\times$ larger radio array proposed as part of the IceCube-Gen2 [8] neutrino observatory.

2. RNO-G station design

RNO-G consists of 35 autonomously powered stations, spaced by 1.25 km to maximise neutrino effective volume. Data transfer and communication is realised via an LTE and LoRaWAN network

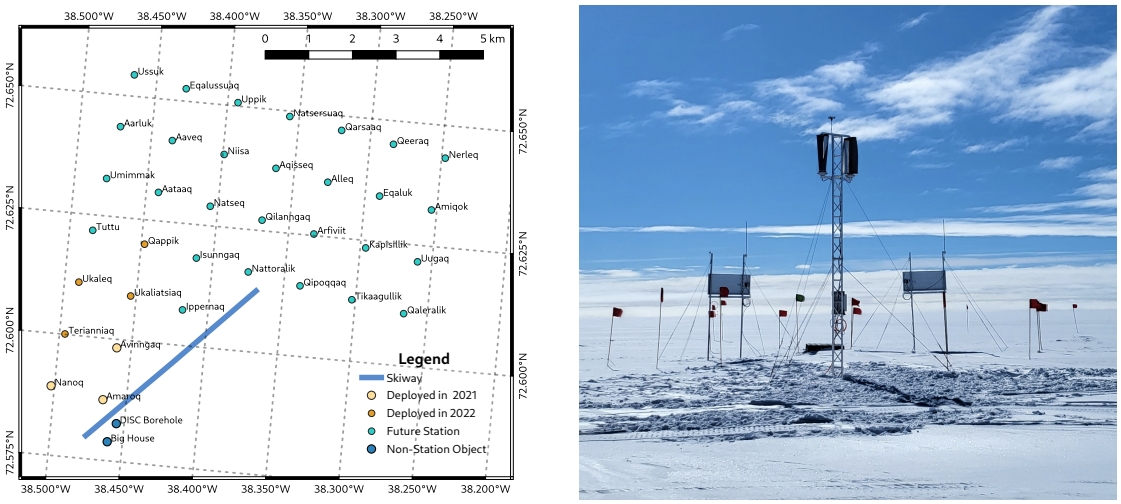

Figure 2: Planned RNO-G array layout at Summit Station with the seven stations already deployed. One of the stations equipped with wind-turbine, Terianniaq, is shown on the right.

with the data server at Summit Station. Fig. 2 shows the footprint of the array and a picture of one of the stations. After the 2022 deployment, seven of the 35 planned stations are now installed and operational. Solar panels allow for continuous data-taking for approximately 8 months per year. In addition, wind-turbines will allow for data-taking also during a large fraction of the winter period. The first iteration of the design consists of two vertical turbines mounted on a mast as shown in Fig. 2. The performance of this turbine design in the field is currently being evaluated at two of the deployed stations.

Each RNO-G station consists of a surface component of nine log-periodic dipole antennas, LPDAs, (three upward, six downward oriented) and a deep component with the remaining 15 channels being vertically (V-Pol) and horizontally (H-Pol) polarized dipole antennas distributed over three 100 m deep air-filled holes. The layout and impressions of the installation process of shallow LPDAs and deep antennas is shown in Fig. 3. The chosen arrangement of antennas is required in order to reconstruct the neutrino direction. It allows for vertex triangulation of the detected signal and to measure the polarization of the signal [15], needed to constrain the orientation of the emission cone and ultimately find the neutrino direction.

On one string, four V-Pol antennas are closely stacked at 100 m depth. These antennas constitute a phased array [16]: signals from individual antennas are coherently summed using a delay-and-sum method at the trigger level, which has a lower threshold than simple coincidence window triggers that have been used previously. The shallow component trigger is realised using a Schottky diode. In 2022, two individual shallow-component trigger channels were tuned to a rate of ~ 0.1 Hz by a 2/3 coincidence on the upward oriented and a 2/6 coincidence on the downward oriented antennas. In addition, every 10 seconds an event is recorded in order to collect a continuous stream of minimum bias data.

When an event is triggered, 640 ns long signal traces are digitized with a sampling rate of 3.2 GHz[1] for all 24 channels within a station. A small sub-sample of the recorded data is directly

[1]In future, the chip can be slowed to 2.4 GHz to extend the recorded time interval.

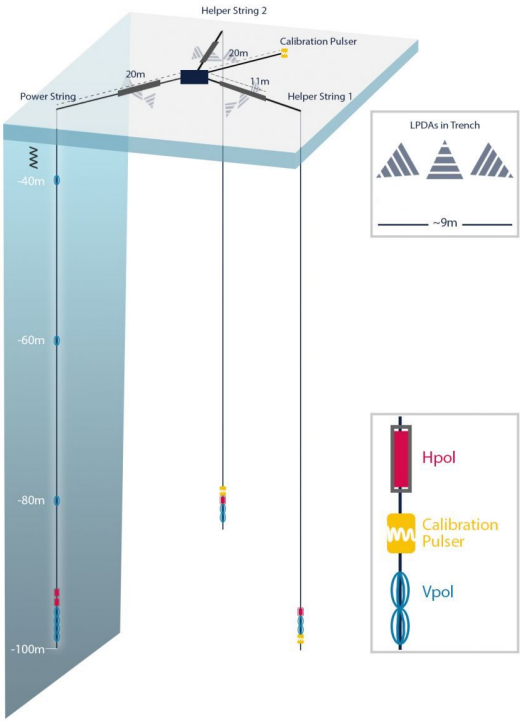

Figure 3: Layout of the hybrid RNO-G station with LPDA antennas deployed in shallow trenches, and V-Pol and H-Pol antennas installed in the deep boreholes. The deployment process for the shallow and deep component, respectively, is illustrated above.

transferred from the data server at Summit Station via satellite. The rest of the data is hand-carried during summer by the field team maintaining detector operation.

3. Deployment progress in 2022

For each of the four new stations deployed in 2022, three 28 cm diameter wide holes were drilled to 100 m depth using the BigRAID depicted in Fig. 4, a custom designed auger drill by the British Antarctic Survey [17]. This season, a tent was added to reduce heat from solar irradiation. Similar to the 2021 deployment season, most holes for the four new stations could be completed in two shifts by two people. Individual drill times ranged from 13 to 20 hours per hole. For the upcoming drilling seasons, we anticipate improvements mainly on the drill head and the control software, and be able to meet the goal that one 100 m hole can be completed in one shift.

After drilling, the deployment team subsequently deployed the deep antenna strings, created trenches for the surface antennas, and installed the data acquisition (DAQ) box and solar panels.

The newly deployed DAQ boxes are equipped with an upgraded power system to allow for the connection of wind turbines. Wind power is needed to increase the livetime fraction of the instrument beyond the promised 2/3 possible with solar panels alone [4] to year round operation. One of the DAQ boxes for the existing stations was also upgraded.

In addition to antenna deployment, the science team determined the antenna positions from the surface with differential GPS, and took various calibration data by pulsing at fixed locations around the stations, from an elevated position at a berm-top at Summit Station, and performed ground-bounce measurements to be able to accurately model the 3 km deep ice sheet at Summit Station.

Figure 4: The British Antarctic Survey's BigRAID auger drill used to drill 11-inch diameter holes *(center)* to a depth of 100 m. The tent *(right)* was added in the 2022 drilling season.

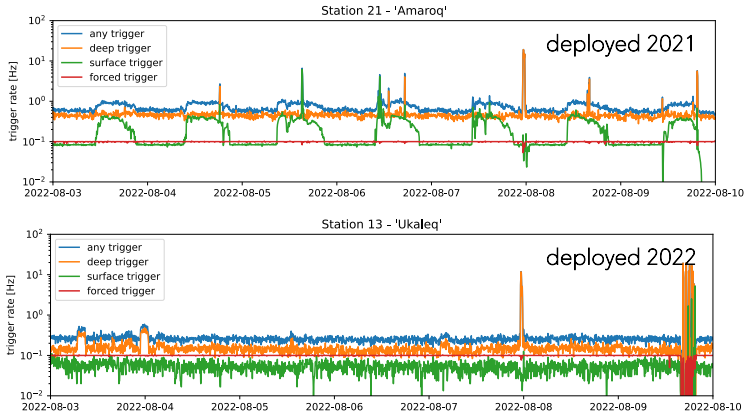

Figure 5: Trigger rates for one week of data-taking for a station deployed in 2021, and a station deployed in 2022 with upgraded power-system and improved EMI protection. For the new station, a series of calibration runs were taken on 2022-08-09.

4. Performance of the deployed stations and observed backgrounds

Already in 2021, the first three RNO-G stations were installed in Greenland. For these stations, two dominant noise sources were present in the surface channels, as visible from the trigger rates in Fig. 5. Surface backgrounds generally are far suppressed in the deep phased array trigger, as is evident from the constant trigger rates in Fig. 5. The surface backgrounds in the stations deployed in 2021 can be attributed to the LoRaWAN communication (occurring at regular 2 min time intervals when data packets are sent from stations to the server), and battery charging noise which dominates the surface trigger rates during daylight. These two backgrounds are effectively suppressed with the newly deployed stations in 2022 (cf. Fig. 5). This is achieved by additional filters and improved EMI shielding in the upgraded DAQ boxes. Additional reducible backgrounds are present in the stations with wind turbine, originating from the turbine's electronics box. These will be prevented with hardware upgrades during the upcoming 2023 field season.

In addition to noise generated by the station electronics itself, various anthropogenic backgrounds are regularly observed in RNO-G. These include intermittent continuous wave signals from weather balloons, air traffic communication, and handheld radio. Snow-mobiles and operation of heavy machinery at Summit Station or the skiway are also visible in nearby stations, and may be filtered for or even exploited as an additional calibration source. To this end, the RNO-G collaboration has access to the logging data for weather balloon flights and snow-mobile traverses

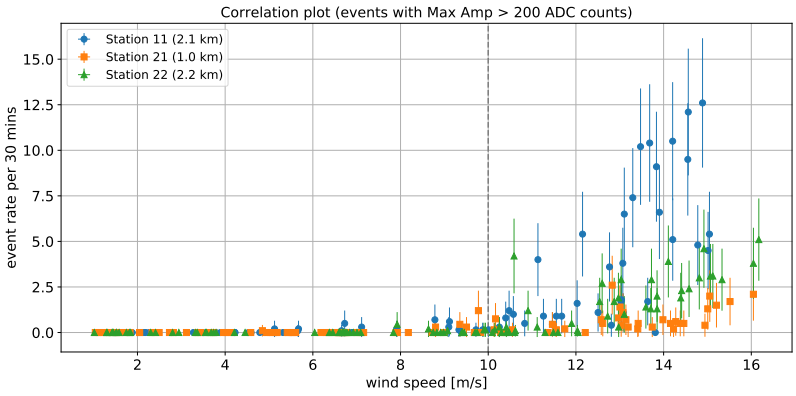

Figure 6: Triboelectric background induced by wind in the surface antennas of RNO-G. Figure taken from Ref. [19].

around Summit Station which use GPS positioning to calibrate the IceSat satellite altimetry data [18]. RNO-G is also storing data from flight tracking and environment variables, like temperatures and wind speeds.

The latter is interesting, since impulsive background events have been observed in various radio neutrino experiments. This so-called triboelectric background with the characteristic empirical threshold at wind speeds exceeding $\sim 10\,\mathrm{m/s}$ is also evident in the surface component of RNO-G, as shown in Fig. 6. Preliminary study of signal direction shows a clustering of arrival directions, which is a possible hint that the (dis)charge might originate from structures installed on the ice [19]. Further study is needed to support this hypothesis.

Besides the mentioned known sources of background, the remainder of the recorded event sample visually agrees with what is expected from noise fluctuations, as is expected when triggering close to the thermal noise floor.

5. Detector calibration

In the following, we highlight the current efforts to calibrate the deployed stations. Precise modelling of the signal response of the instrument is a necessary prerequisite for physics analysis.

The initial antenna positions are determined via differential GPS to few centimeter precision on the firn surface. In addition, the deployed depths of the deep antennas are determined via tape measure. More refined calibration of the positioning and time delays (already accounting for the fibre and cable delays measured in the lab) can be performed using the data taken by the science team when pulsing from known GPS positions around the stations and from an elevated position from a berm-top at Summit Station.

In addition, calibration runs have been taken for all stations with one of the two in-situ calibration pulsers deployed in the boreholes activated at a time. One event from a calibration run when pulsing from one of the 'helper' strings of station Amaroq is shown in Fig. 7.

Bias voltage scans are recorded to map the ADC counts of the digitized signal to voltage values, which is close to linear unless for large signal amplitudes. The amplifier response in the DAQ box shows some dependence on temperature. Few weeks after deployment, when the DAQ box is covered with snow the temperature however stabilizes. The precise method for ADC to voltage conversion is still being worked on.

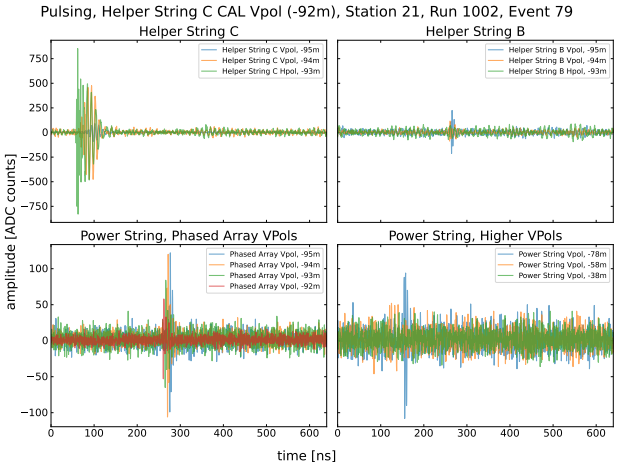

Figure 7: Calibration pulses triggered on the power string as seen in the two helper strings (top row), the V-Pol antennas of the phased array (bottom left) and V-Pols at shallower depth (bottom right) on the power-string. The emitting antenna is located above the detection channels of 'Helper String C'.

6. Outlook to 2023 and first physics results

While current efforts are concentrating on calibrating the deployed stations, reconstruction algorithms using the signal from the deep antennas are in place for neutrino energy [21] as well as direction [15]. An algorithm developed with an ARIANNA-like arrangement of shallow antennas [22] can be used also for the reconstruction of neutrino candidates with the downward oriented LPDAs in RNO-G.

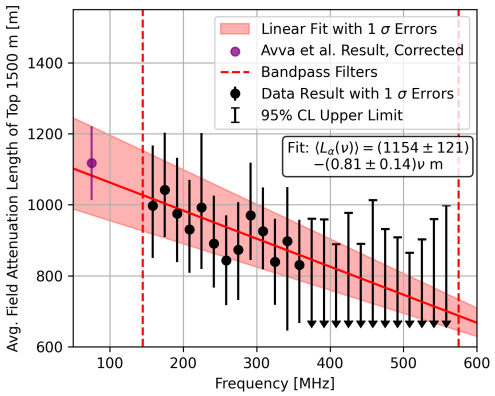

Figure 8: Attenuation length measurement. Figure taken from Ref. [20].

A cosmic-ray search is under development [7] that is searching for CR candidate events by correlating the recorded data traces of the upward-pointing LPDAs with the template expectation for noiseless impulsive signals after convolution with the RNO-G hardware response. RNO-G is already expected to have collected several cosmic-ray events in the recorded dataset that will be found when applying the analysis to the full data-set on disk, even assuming a conservative detection threshold [6].

In-ice radio signals of CR shower cores which have not fully developed in air [23], and secondary showers induced by UHE prompt atmospheric muons [24], as well as the refracted in-air CR signal propagating to the deep antennas [25] will also be searched for in the future.

RNO-G may also be able to detect the diffuse thermal radio emission from our Galaxy. This is however complicated by the temperature dependence of the amplifier response, and the location on the northern hemisphere, meaning that the central region of the galactic plane is below or close to the horizon, and hence requires careful analysis.

The first RNO-G physics result published [20] used ground-bounce data collected at Summit Station in 2021 for a depth-dependent attenuation measurement of the radio signal in the ice sheet below Summit Station. The bulk ice attenuation length shown in Fig. 8 could be extracted taking into account the chemical composition of the ice.

To allow for improvements in the drill to reach the goal of being able to drill one hole per shift, and hardware integration and lab calibration measurements, the next drilling season is planned only for 2024. Next year, 2023, will be used to service and upgrade the existing stations, including the wind-turbine electronics, and take additional measurements for calibration and ice studies. Most importantly however, all seven operating stations are expected to resume data-taking after the winter and collect data for cosmic ray studies and to start searching for the first radio neutrino yet to be detected.

References

[1] IceCube collaboration, *Science* **342** (2013) 1242856 [1311.5238].

[2] IceCube collaboration, *Science* **361** (2018) 147–151 [1807.08794].

[3] IceCube collaboration, *Science* **378** (2022) 538–543.

[4] RNO-G collaboration, *JINST* **16** (2021) P03025 [2010.12279].

[5] S. Barwick and C. Glaser, *Radio Detection of High Energy Neutrinos in Ice*, (2022) [2208.04971].

[6] L. Pyras and I. Plaisier for the RNO-G collaboration, *PoS* (ECRS2022) 088.

[7] J. Henrichs for the RNO-G collaboration, *these proceedings*, *PoS* (ARENA2022) 007.

[8] IceCube-Gen2 collaboration, *PoS* **ICRC2021** (2021) 1183 [2107.08910].

[9] IceCube collaboration, *The Astrophysical Journal* **928** (2022) 50.

[10] A. Anker et al., *White Paper: ARIANNA-200 high energy neutrino telescope*, (2020) [2004.09841].

[11] X. Rodrigues, J. Heinze, A. Palladino, A. van Vliet and W. Winter, *Phys. Rev. Lett.* **126** (2021) 191101 [2003.08392].

[12] P. Padovani, M. Petropoulou, P. Giommi and E. Resconi, *Mon. Not. Roy. Astron. Soc.* **452** (2015) 1877–1887 [1506.09135].

[13] K. Fang, K. Kotera, K. Murase and A.V. Olinto, *Phys. Rev. D* **90** (2014) 103005 [1311.2044].

[14] M.S. Muzio, M. Unger and G.R. Farrar, *Phys. Rev. D* **100** (2019) 103008 [1906.06233].

[15] I. Plaisier for the RNO-G collaboration, *these proceedings*, *PoS* (ARENA2022) 007.

[16] P. Allison et al., *Nucl. Instrum. Meth. A* **930** (2019) 112 [1809.04573].

[17] J. Rix, R. Mulvaney, J. Hong and D. Ashurst, *Journal of Glaciology* **65** (2019) 288–298.

[18] K. Brunt et al., *The Cryosphere Discussions* **11** (2016) 681–692.

[19] J.A. Aguilar et al., *Astroparticle Physics* **145** (2023) 102790.

[20] J.A. Aguilar et al., *Journal of Glaciology* **68(272)** (2022) 1234–1242.

[21] J.A. Aguilar et al., *Eur. Phys. J. C* **82** (2022) 147 [2107.02604].

[22] G.G. Gaswint, *Quantifying the Neutrino Energy and Pointing Resolution of the ARIANNA Detector*, Ph.D. thesis, UC, Irvine, 2021.

[23] S. de Kockere, *these proceedings*, *PoS* (ARENA2022) 015.

[24] D. García-Fernández, A. Nelles and C. Glaser, *Phys. Rev. D* **102** (2020) 083011.

[25] U. Latif, *these proceedings*, *PoS* (ARENA2022) 016.

PoS(ARENA2022)005

Full Author List: RNO-G Collaboration

J. A. Aguilar[1], P. Allison[2], D. Besson[3], A. Bishop[4], O. Botner[5], S. Bouma[6], S. Buitink[7], M. Cataldo[6], B. A. Clark[8], K. Couberly[3], Z. Curtis-Ginsberg[9], P. Dasgupta[1], S. de Kockere[10], K. D. de Vries[10], C. Deaconu[9], M. A. DuVernois[4], A. Eimer[6], C. Glaser[5], A. Hallgren[5], S. Hallmann[11], J. C. Hanson[12], B. Hendricks[13], J. Henrichs[11,6], N. Heyer[5], C. Hornhuber[3], K. Hughes[9], T. Karg[11], A. Karle[4], J. L. Kelley[4], M. Korntheuer[1], M. Kowalski[11,14], I. Kravchenko[15], R. Krebs[13], R. Lahmann[6], U. Latif[10], J. Mammo[15], M. J. Marsee[16], Z. S. Meyers[11,6], K. Michaels[9], K. Mulrey[17], M. Muzio[13], A. Nelles[11,6], A. Novikov[18], A. Nozdrina[3], E. Oberla[9], B. Oeyen[19], I. Plaisier[6,11], N. Punsuebsay[18], L. Pyras[11,6], D. Ryckbosch[19], O. Scholten[10,20], D. Seckel[18], M. F. H. Seikh[3], D. Smith[9], J. Stoffels[10], D. Southall[9], K. Terveer[6], S. Toscano[1], D. Tosi[4], D. J. Van Den Broeck[10,7], N. van Eijndhoven[10], A. G. Vieregg[9], J. Z. Vischer[6], C. Welling[9], D. R. Williams[16], S. Wissel[13], R. Young[3], A. Zink[6]

[1]ULB Brussels, Université Libre de Bruxelles, Science Faculty CP230, B-1050 Brussels, Belgium
[2]Ohio State University, Dept. of Physics, Center for Cosmology and AstroParticle Physics, Ohio State University, Columbus, OH 43210, USA
[3]University of Kansas, University of Kansas, Dept. of Physics and Astronomy, Lawrence, KS 66045, USA
[4]University of Wisconsin-Madison, Wisconsin IceCube Particle Astrophysics Center (WIPAC) and Dept. of Physics, University of Wisconsin-Madison, Madison, WI 53703, USA
[5]Uppsala University, Uppsala University, Dept. of Physics and Astronomy, Uppsala, SE-752 37, Sweden
[6]Friedrich-Alexander-University Erlangen-Nürnberg, Erlangen Center for Astroparticle Physics (ECAP), Friedrich-Alexander-University Erlangen-Nürnberg, 91058 Erlangen, Germany
[7]VUB Brussels, Vrije Universiteit Brussel, Astrophysical Institute, Pleinlaan 2, 1050 Brussels, Belgium
[8]Michigan State University, Dept. of Physics and Astronomy, Michigan State University, East Lansing MI 48824, USA
[9]University of Chicago, Dept. of Physics, Enrico Fermi Inst., Kavli Inst. for Cosmological Physics, University of Chicago, Chicago, IL 60637, USA
[10]Vrije Universiteit Brussel, Vrije Universiteit Brussel, Dienst ELEM, B-1050 Brussels, Belgium
[11]DESY, Deutsches Elektronen-Synchrotron DESY, Platanenallee 6, 15738 Zeuthen, Germany
[12]Whittier College, Whittier College, Whittier, CA 90602, USA
[13]Penn State University, Dept. of Physics, Dept. of Astronomy & Astrophysics, Penn State University, University Park, PA 16801, USA
[14]HU Berlin, Institut für Physik, Humboldt-Universität zu Berlin, 12489 Berlin, Germany
[15]University of Nebraska-Lincoln, Dept. of Physics and Astronomy, Univ. of Nebraska-Lincoln, NE, 68588, USA
[16]University of Alabama, Dept. of Physics and Astronomy, University of Alabama, Tuscaloosa, AL 35487, USA
[17]Radboud University, Dept. of Astrophysics/IMAPP, Radboud University, PO Box 9010, 6500 GL, The Netherlands
[18]University of Delaware, Dept. of Physics and Astronomy, University of Delaware, Newark, DE 19716, USA
[19]Ghent University, Ghent University, Dept. of Physics and Astronomy, B-9000 Gent, Belgium
[20]University of Groningen, Kapteyn Institute, University of Groningen, Groningen, The Netherlands

PoS(ARENA2022)005